Unidirectional Photoisomerization of Styrylpyridine for Switching the Magnetic Behavior of an Iron(II) Complex: A MLCT Pathway in Crystalline Solids

Antoine Tissot,[†] Marie-Laure Boillot,*[,†] Sébastien Pillet,[‡] Epiphane Codjovi,[§] Kamel Boukheddaden,[§] and Latévi Max Lawson Daku[||]

ICMMO, ECI, UMR CNRS 8182, Université Paris-Sud, 15 Rue Georges Clémenceau, 91405 Orsay, France, CRM2, UMR CNRS 7036, Institut Jean Barriol, Nancy-Université, BP239, 54506 Vandoeuvre les Nancy, France, GEMAC, UMR 8635, Université de Versailles-Saint Quentin en Yvelines, 45 Avenue des Etats-Unis, 78035 Versailles Cedex, France, and Faculté des Sciences, Université de Genève, 30 Quai Ernest-Ansermet, CH-1211 Genève, Switzerland

Received: July 15, 2010; Revised Manuscript Received: October 22, 2010

The photoreactivity of two iron(II)−styrylpyridine frameworks $Fe(stpy)_4(NCSe)_2$ (stpy = 4-styrylpyridine) has been investigated for the very first time in a crystalline solid. A quantitative cis-to-trans isomerization of stilbenoids is shown to occur in the confined environment of the inorganic solid. The photochromic reaction was driven by a visible excitation into the metal-to-ligand charge transfer absorption of the high-spin all-cis complex. The solid-state transformation is accompanied by a unit-cell volume increase and an amorphization. Interestingly, the photoproduct formed by irradiating the high-spin all-cis reactant undergoes a spin conversion when the temperature is decreased. This observation is related to the "ligand-driven light-induced spin change" effect in a constrained environment.

I. Introduction

Performing switching operations via optical stimuli is an approach of growing importance in the field of molecular magnetism and solid-state science. For this challenging task, spin-crossover solids[1] constitute well-known and extensively studied model materials. The reversible switching of a transition metal ion between high-spin (HS) and low-spin (LS) electronic states, which occurs under an external perturbation, is one spectacular feature of the spin-crossover phenomenon.[1] Most of the physical properties of a spin-crossover material (such as magnetic, optical, structural, or dielectric properties) change along with the spin state switching process, which may be triggered by several stimuli.[2] This fundamental property first encountered in molecular magnetic materials arouses a lot of interest as the bistability of a number of strongly cooperative spin-transition solids offers great potentialities in molecular electronics (display, memory devices, ...).[3]

At temperatures well below the thermal spin-crossover range, excitation of these solids within MLCT (metal-to-ligand charge transfer) or metal-centered (ligand-field) absorption bands leads to a quantitative LS to HS conversion via a lengthening of the metal−ligand bond distances. This effect called light-induced excited spin state trapping (LIESST), discovered by Hauser and co-workers, is well documented for Fe^{II} spin-crossover materials.[4]

In the ligand-driven light-induced spin change effect (LD-LISC),[5,6] the synergetic combination of two moieties−selected iron(II) coordination cores of spin-crossover type and stilbenoid ligands−was proposed by Zarembowitch to elaborate a high-temperature photoswitchable system in which the HS ↔ LS conversion of the metal ion would be reversibly triggered by the ligand photoisomerization. Accordingly the spin-state stability is controlled by the energy barrier between the ligand configurational isomers.[7] Potential applications of LD-LISC molecular systems may be expected in the field of photomagnetic (or optical) memories and optical signal processing. Since these pioneering works, the field of photomagnetic materials has grown with a variety of systems (molecules, coordination networks, hybrid materials) and processes (charge transfer, valence tautomerism, photochromism, ...).[8]

Stilbenoid compounds are found in several areas of applications including technological materials.[9,10] When incorporated as ligands in functional coordination compounds, the metal center can play an active role in the photochemistry of the stilbenoid chromophore, or conversely its characteristics can be modulated by the stilbenoid properties.[11] Stilbenoids are strong UV absorbers and consequently the elaboration of highly diluted materials is required to study their light-induced reactivity. The LD-LISC compounds may be processed in matrices, like thick polymeric films[5b] and Langmuir−Blodgett films,[12] since the effect is of molecular nature. Thus for the two complexes $Fe^{II}(stpy)_4(NCSe)_2$ (stpy = *cis*- or *trans*-4-styrylpyridine) dispersed into PMMA thin films, the cis ↔ trans (or Z/E) ligand-centered photoisomerization was induced under UV and the concomitant switching of their magnetic behaviors was demonstrated.[13,14]

Z/*E* isomerization of stilbenoids requires large spatial voids, which constitutes a strong disadvantage for a reaction in crystals.[15] Nevertheless, the literature provides some examples of selective isomerization processes in volume-confined media and such processes are especially important in biology.[16] The one bond flip process (double bond twist) is the mechanism favored in solution, while the volume-conserving hula-twist process (concerted twist of adjacent double and single bonds) has been recognized in constrained media[17] and even in the gas phase.[18] Cis-to-trans isomerization of retinal within the rhodopsin proteins is an example of a unidirectional, efficient, and selective

* marie-laure.boillot@u-psud.fr.
[†] Université Paris-Sud.
[‡] Nancy-Université.
[§] Université de Versailles-Saint Quentin en Yvelines.
[||] Université de Genève.

10.1021/jp106583f
Published on Web 11/12/2010

hula-twist process.[16] Alternatively, single-crystal-to-single-crystal *E*/*Z* isomerization processes have been recognized in different molecular materials, where they appear as being controlled by the location of void volumes with respect to the trajectories of the photoactive function.[19−21] Kaupp et al. have reported the *E*/*Z* isomerization of crystalline (*Z*)-2-benzylidene butyrolactone, which proceeds via a supramolecular and collective phase rebuilding mechanism.[20] In the analysis of the single-crystal-to-single-crystal *E*/*Z* isomerization of Zn-coordinated tiglic acid, Coppens et al. have related the kinetics of the isomerization to the effect of the crystalline environment.[21]

In relation with these works, X-ray single-crystal diffraction measurements previously carried out on crystalline samples of $Fe^{II}(stpy)_4(NCSe)_2$ brought out interesting characteristics (free-cavities, packing, absence of $\pi-\pi$ stacking interactions, ...) which might suggest some degrees of freedom and reactivity in the two lattices. We report here the existence of a photoswitching pathway of these colored crystalline solids using visible light. Different optical, structural, and vibrational investigations were undertaken in order to probe the photoisomerization process in such a confined environment and its consequence on the spin state of the metal center.

II. Experimental Section

Syntheses and Crystallizations. The two isomers of $Fe(stpy)_4(NCSe)_2$ were synthesized and characterized as previously reported.[14] Single crystals were isolated by slow evaporation of a MeOH:H_2O solution of all-trans (red, trans-isomer of stpy) and all-cis complexes (orange, cis-isomer of stpy).

ATR-IR Spectrometry. Attenuated total reflection infrared spectra measurements were performed with a IFS-66 spectrometer. Pellets of $Fe(stpy)_4(NCSe)_2$ (diameter 5 mm, thickness ~1 mm) were obtained by pressing the powder under 2 kbar for 3 min, using an optical polished piston. Irradiations were carried out at 532 nm with a Nd:YAG laser (~25 mW/cm^2) or with a black lamp (λ_{max} = 365 nm).

Ellipsometry. Spectroscopic ellipsometry (SE) measurements were carried out at room temperature on pellets of $Fe(stpy)_4(NCSe)_2$ prepared as described above. The measurements were performed in the 260−800 nm optical range at an incident angle of 70° (near the Brewster's angle), using the UVISEL spectroscopic phase modulated ellipsometer[22] in which the light source was a 150 W Xe short arc lamp. The diameter light spot on the sample was of ~3−4 mm and the recording time was 3 min for each spectrum. Figure S1 (Supporting Informations) shows the ellipsometric refractive index $n(\lambda)$ (all-cis compound after photoexcitation) determined at room temperature from the wavelength dependences of the ellipsometric parameters Ψ and Δ. The consistency of the ellipsometric spectra was checked through the analysis of the Kramers−Kronig (KK) relations[23] between the refractive index, $n(\lambda)$, and the extinction coefficient, $k(\lambda)$, as in ref 24 (see the Supporting Informations).

Reflectivity. Diffuse reflectance measurements have been performed at variable temperature with an already described setup.[25] The light source was a 100 W QTH (Quartz Tungsten Halogen) lamp with an interferential filter located ahead of the optical fibers, which carry light to the sample. It was checked that the $\lambda = 650 \pm 50$ nm wavelength optimizes the sample analysis as the sample reactivity is much lower than in the 550 nm range. The sample photoexcitation was performed with an ex situ λ = 532 nm Nd:YAG laser. Typical intensity was 15 mW/cm^2.

X-ray Diffraction. Kinetic X-ray diffraction measurements under laser excitation have been conducted at room temperature. First, a very thin layer, not exceeding 20−50 μm in thickness, of microcrystalline powder of the all-cis complex has been deposited on a low background substrate. The procedure and experimental setup for kinetic powder photocrystallographic experiments have already been reported.[26] The sample was then illuminated with a frequency doubled Nd:YAG laser (λ = 532 nm) coupled to an optical fiber. A second data set was measured after 30 min laser exposure and a third one after 120 min exposure. In a separate experiment, single-crystal photocrystallographic analysis has been performed with an Oxford Diffraction Supernova diffractometer with Mo Kα radiation. A complete data set was measured at room temperature as a reference on a 200 μm single crystal. Continuous photoexcitation was then applied during the diffraction measurements, using a Spectra Physics Stabilité 2018 Ar−Kr gas laser (λ = 534 nm) coupled to an optical fiber. The unit-cell parameters (Table S1, Supporting Information) were derived along the photoexcitation. We observed that the intensity of the diffraction Bragg spots gradually decreases as the laser exposure time increases, so that after nearly 60 min of laser illumination, the diffraction spots were barely visible. The experiment was reproduced on a second sample, and the laser illumination was stopped after 50 min. A complete diffraction data set, albeit of limited quality was then measured for structure determination purposes (further experimental details are given in the Supporting Informations).

Magnetic Measurements. Magnetization measurements were carried out with a Quantum Design SQUID magnetometer (MPMS5S Model) calibrated against a standard palladium sample. The magnetization vs temperature data were collected in the 5−300 K temperature range within H = 5000 Oe. For photoexcitation of solids, the magnetometer was equipped with an optical fiber (UV grade fused silica) connected to a Nd:YAG pulsed laser Surelite-Continuum Performance (ranging from 450 to 800 mJ at 1064 nm and harmonic options for 532, 355 nm outputs). In situ excitations were performed with λ = 532 nm (~25 mW/cm^2).

Computational Details. The geometries and frequencies of the cis- and trans-isomers of 4-styrylpyridine have been determined in the S_0 and T_1 states. The calculations have been performed within DFT[27] with the NWChem program[28] package, using the B3LYP functional[29] and the DFT DZVP basis set of double-ζ polarized quality.[30] The frequency calculations performed within the harmonic approximation show that the optimized geometries are true minima because no imaginary frequency was found. For the trans-isomer, the molecular symmetry was constrained to C_s during the calculations.

III. Results

We will first briefly recall the structural and magnetic properties of the parent crystalline solids before presenting their optical properties. Then, we will focus on the impact of light irradiation on the stpy photoactive moiety, its subsequent influence on the properties of the Fe^{II} coordination center itself, and the computational results obtained for the preliminary characterization of 4- styrylpyridine in its ground and excited T_1 states.

1. Properties of the Parent Crystalline Solids. ***a. Molecular Structures, Magnetic Behavior.***[13,14] For both molecular species (i.e., all-cis and all-trans isomers), the Fe(II) ions lie in pseudo-octahedral environments with two nitrogen atoms of the NCSe ligand in the axial position and four nitrogen atoms of the pyridine rings in the equatorial plane. The evolution of these

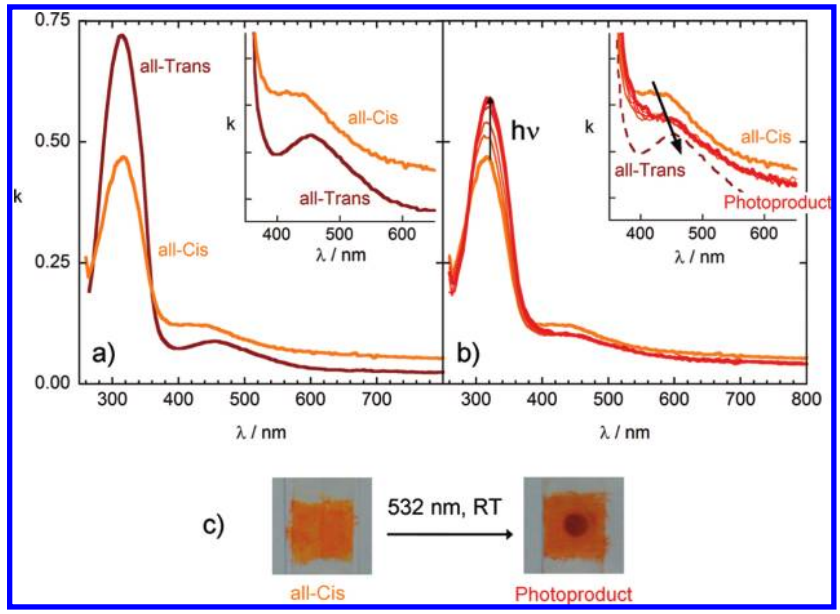

Figure 1. (a) Room temperature ellipsometric spectra of the extinction coefficient, k, for all-trans and all-cis compounds in the form of pellets. (b) Evolution of the spectrum of all-cis complex upon irradiation ($\lambda_{exc} = 532$ nm). Insets: Expansions of the curves in the 350−600 nm range. (c) Photos of powder of all-cis compound before and after irradiation.

bond lengths by lowering the temperature from 293 to 104 K closely reflects the spin crossover of the all-trans complex and the HS ground state of the all-cis complex, in agreement with the magnetic behavior. The cohesion of both solid structures is achieved by numerous and weak intermolecular contacts (involving Se(NCSe) and aromatic groups); no intermolecular π-stacking with a parallel configuration is found. Interestingly, the change in molecular volumes (unit cell volume per metal ion) corresponding to the formal substitution of a *cis*-stpy isomer by the trans one is rather small (3.4% at 293 K, 0.95% at 104 K), suggesting that the *Z*/*E* change would possibly lead to unit-cell reorganizations comparable to the spin-crossover ones. The analysis of free-cavities volumes shows the presence of large fractions of void spaces (ca. 11% at $r = 0.8$ Å) in the crystal packing for both all-cis and all-trans complexes.

The magnetic properties of microcrystalline solids are determined closely by the stpy configurations. The $\chi_M T$ vs T curves (χ_M being the molar magnetic susceptibility, T the temperature) show a spin-crossover behavior for the all-trans species ($T_{1/2} = 163$ K) and a HS ground state for the all-cis complex.

b. Optical Properties of Crystalline Solids. In Figure 1a, the room temperature (RT) spectra of both solids present similar features: a very intense UV absorption, which closely depends on the ligand *Z*/*E* configuration and a weaker absorption in the visible range. These data are comparable to those collected with the doped PMMA thin films.[13,14] For the all-trans compound, the very intense UV band (at 315 nm) is directly identified as the intraligand (IL) $\pi-\pi^*$ transitions of the coordinated *trans*-stpy ($k = 0.72$) (at ca. 313 nm in the PMMA thin film). The UV absorption of the all-cis complex is also assigned to the $\pi-\pi^*$ transitions of *cis*-stpy ($k = 0.47$) despite an unusual red-shift with respect to the absorption energies of the complexes (or free-base ligands) in PMMA films and in solutions.

One characteristic of the *cis*-stpy isomer is its large conformational flexibility[31] that contributes, in addition to vibrational and solvent effects, to broaden the $\pi-\pi^*$ absorption of weaker intensity, occurring at high energy for solutions and PMMA thin films (ca. 279 nm). In contrast, the crystal structure of the studied all-cis molecule shows the trapping of four well-defined *cis*-stpy geometries around the Fe^{II} ions that results from specific packing effects related for example to close contacts between pyridyl, phenyl, and ethylenic groups.[14] These features corroborate the present observation of a more intense and narrower absorption shifted with respect to the solution data.

In the inset of Figure 1a, the vis absorption bands observed at ca. 455 ($k = 0.089$) and 435 nm ($k = 0.123$) for all-trans and all-cis complexes, respectively, are typical for Fe(3d) → π^*(stpy) metal-to-ligand charge transfer (MLCT) transitions of HS iron(II) ions.[32] The change of the crystals coloration from orange (all-cis compound) to red-bordeaux (all-trans compound) is directly related to the characteristics of the MLCT absorptions.

2. Solid-State Photochromism. ***a. Nature of the Photoproduct Obtained by Vis Excitation: Spectroscopic Signature of the Cis−Trans Isomerization.*** When irradiated by UV light ($\lambda = 365$ nm, IL transition, RT), the solid interface of all-cis (all-trans) species suffers minor (no) alteration (see Figure S2, Supporting Informations). These observations are consistent with the very low penetration depth δ of UV light shown by our ellipsometric data (for example $\delta \approx 50$ nm in the $\pi\pi^*$ absorption band of the all-cis compound).[33] A 6-fold longer penetration depth is expected in the vis range wherein the MLCT transitions occur (see Figure 1a).

As depicted in Figure 1c, irradiating the orange all-cis sample at 550 nm produces a thermally stable red sample in the unmasked area. A 650 nm light leads to similar changes but the evolution is considerably slowed down. Finally, irradiation of the red all-trans sample does not show any effect.

The evolution under vis irradiation of the all-cis compound was quantitatively monitored by room temperature ellipsometric measurements (in Figure 1b). The comparison of spectra indicates the presence of an isosbestic point (ca. 288 nm) in the UV range as well as large intensity changes in the bands previously assigned to $\pi\pi^*$ ligand-localized transitions; these features suggest a cis-to-trans isomerization of the stpy chromophores. The intensity of these $\pi\pi^*$ transitions reaches a saturation regime after 30 min of irradiation time. The associated Fe(3d) → π^*(stpy) charge transfer band becomes weaker, broadened, and slightly red-shifted (see the inset in Figure 1b) with respect to the starting material. These features may be accounted for by (i) the preservation of the metal ion in the HS

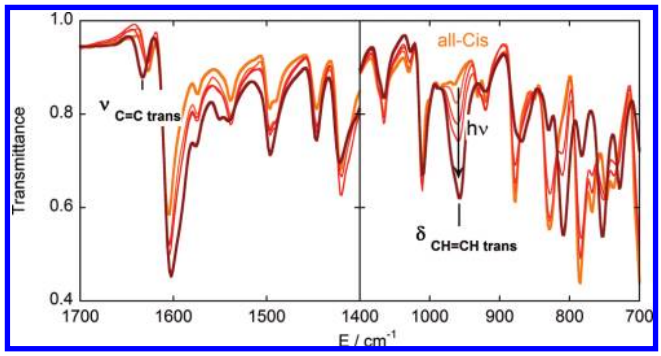

Figure 2. ATR-IR characterizations of the all-cis species (orange spectrum) and its evolution during the vis excitation of the solid pellet at room temperature.

state at room temperature (more intense MLCT absorptions are typical for LS Fe^{II} species), (ii) the formation of complexes with different isomers of *cis*- and *trans*-stpy, and (iii) the progressive disorganization of the molecule environment (formation of an amorphous solid as will be shown below by X-ray). The low-energy excitation of the all-cis compound raises the questions of (i) a possible overlap between $\pi\pi^*$ and MLCT transitions and (ii) the wavelength dependence of the process. As mentioned above, the photochromic reaction is still detected by IR measurements when the sample was exposed to a 650 nm irradiation, a wavelength at which no $\pi\pi^*$ transition should occur.

To obtain a better insight into the transformation, we have performed an ATR-IR characterization of the all-cis and the photogenerated samples. The RT spectra in Figure 2 show several vibrational modes in the 1650−600 cm^{-1} range that are changed in both intensity and energy. Along with the transformation, the intensity of those bands characteristic of the all-cis compound, located at 883, 832, 789, and 700 cm^{-1} (CH deformations), strongly decreases whereas the band at 1628 cm^{-1} (ethylenic C═C stretching) is shifted. In parallel, strong vibrational bands, which are also identified in the spectrum of the pure all-trans compound, appear at 1633 (ethylenic C═C stretching), 957 (CH out-of-plane deformation of trans CH═CH), and 809 and 755 cm^{-1} (CH deformations). The observation of distinctive frequencies of the trans isomer, in addition to the solid color change and the gain in intensity of $\pi\pi^*$ transitions, demonstrates the formation of *trans*-stpy isomers and thus the occurrence of a cis-to-trans isomerization (a conversion of ∼66%, from the relative area variation under the IR absorption bands). In fact, this photoreaction influences the whole inorganic system: weaker variations are observed in the NC stretching frequencies of the NCSe groups (Figure S3, Supporting Informations), as well as of the pyridine rings. This feature can be understood as the consequence of the attendant structural and electronic reorganization, including the change of the complex symmetry. Given that the NC_{NCSe} stretching vibration of the photoproduct is observed at 2051 cm^{-1} (2057 cm^{-1} for the all-cis species), we can draw the conclusion that the iron center of the photogenerated compound is still in the HS state; a frequency of ca. 2099 cm^{-1} is indeed expected for a LS state.[34] Finally, we note that no side reaction (like photocyclization, photodimerization, and ligand decoordination) is detected.

This set of data proves that a visible excitation of the all-cis species is suitable for isomerizing the *cis*-styryl group in the crystalline solid; this transformation affects the organic and inorganic moieties but at RT, the metal ions in both species (all-cis complex and photoproduct) are found in the HS state. The fact that the excitation wavelength at 550 nm corresponds to the low-energy side of the MLCT transitions suggests the existence of an isomerization pathway through the initial excitation of a ^{5}MLCT excited state.

b. Transformation in the Confined Environment of the Crystal: X-ray Diffraction Investigation. This solid-state transformation raises the question of how does the crystal accommodate the structural changes brought about by the cis-to-trans photoisomerization. We have thus performed photocrystallographic measurements on microcrystalline powder as well as on single crystals.

The reference powder diffraction pattern (Figure 3) for the all-cis reactant exhibits sharp peaks whose 2θ positions are consistent with the positions predicted from the all-cis crystal structure at RT.[14] Upon laser exposure, the peak intensities progressively decrease but a very broad feature grows, centered around $2\theta = 20°$. After 120 min of laser exposure, the sharp peaks have become very weak and the phototransformation is almost complete. Along with their loss of intensity, the peaks shift toward lower 2θ angles (Figure 3b), indicating a unit-cell volume increase. These data clearly show that the disappearing all-cis phase is structurally perturbed by the environment modification.

In view of these results, we can propose a simple scenario of the phototransformation mechanism, which is illustrated on Figure 4b. The material progressively transforms from a crystalline all-cis phase to an amorphous photoproduct phase through crystal disintegration. While the transformation proceeds, the disappearing all-cis material undergoes a gradual unit-cell volume expansion as more and more molecules are converted to the photoproduct species. This is indicative of a nontopotactic solid-state reaction, possibly with large molecular reorganizations.[20b] A topotactic reaction is controlled by the crystal lattice and structural topology of the reactants, it would thus preserve the structural organization and crystal lattice, without large molecular movements; crystal disintegration is usually considered as a signature of nontopotaxy. Hereafter, the disappearing all-cis reactant crystalline phase, which we characterize by X-ray diffraction, will be denoted the "photo-perturbed crystalline phase". However, no structural information can be derived from this diffraction analysis on the amorphous photoproduct, especially with regards to the configuration of the stpy ligands.

To further quantitatively characterize these transformations, single-crystal diffraction measurements under continuous laser excitation have been performed.

According to the progressive crystal disintegration found in the powder diffraction measurements, it is observed that, while the laser excites the sample, the diffraction Bragg peaks continuously decrease in intensity and disappear after 60 min of laser illumination. In parallel, the evolution of the unit-cell volume was derived as a function of laser exposure (Figure 4) and shows a continuous increase from 4780 $Å^3$ (all-cis reactant solid) to ca. 4829 $Å^3$, which can be estimated as 49 $Å^3$ (unit cell expansion ∼1%); this is in line with the peak position shift deduced from the powder diffraction data. The amorphization was further confirmed by recording pictures of the crystal under a polarized microscope (crossed-polarizers in transmission mode). Neat extinction conditions were observed before photoirradiation, while the sample after photoirradiation did not show extinction conditions any more. The photocrystallographic experiment was repeated on a second sample, but this time, the illumination was stopped before the complete amorphization of the material. This offers the possibility to analyze the crystal structure of the material close to the complete photoconversion

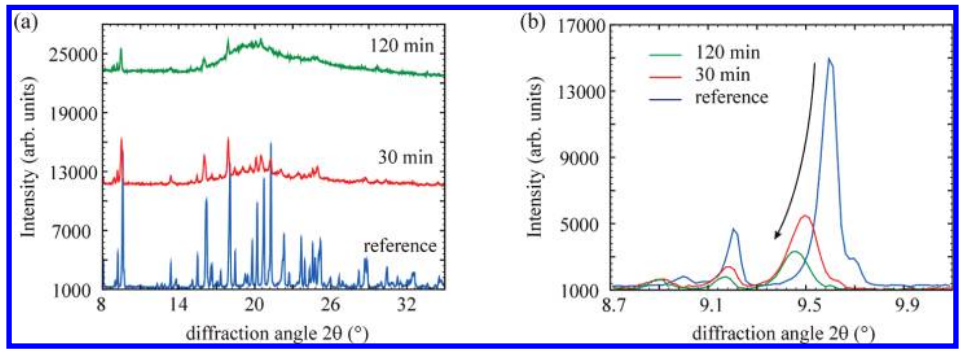

Figure 3. (a) Superposition of the reference all-cis reactant (bottom), 30 min exposure (middle), and 120 min exposure (top) powder diffraction patterns. The scans are vertically displaced for clarity. (b) Superposition of the diffraction patterns in the [8.7−10.1°] 2θ range.

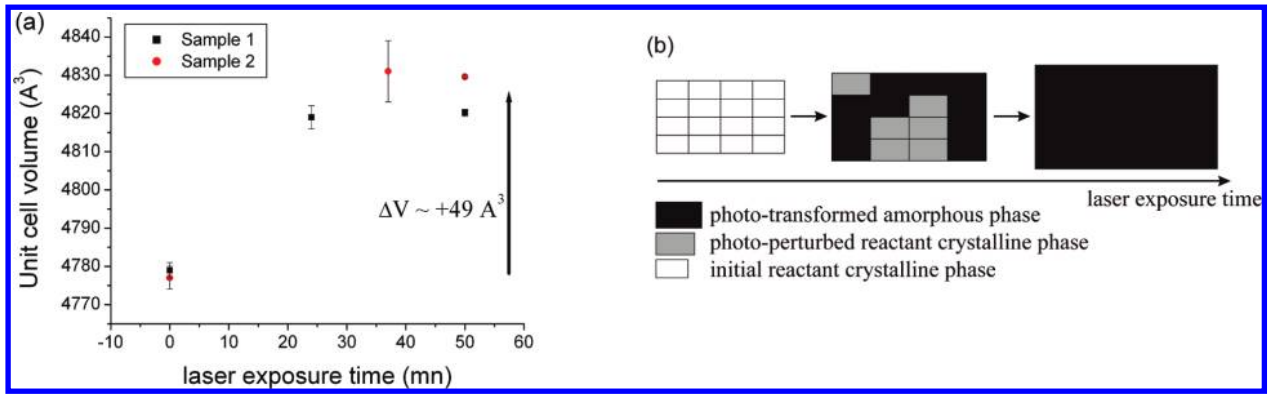

Figure 4. (a) Evolution of the unit cell volume as a function of laser exposure for the all-cis species. The measurements have been made on two separate samples 1 and 2 (see the Experimental Section for more explanations). (b) Schematic view of the structural phototransformation mechanism.

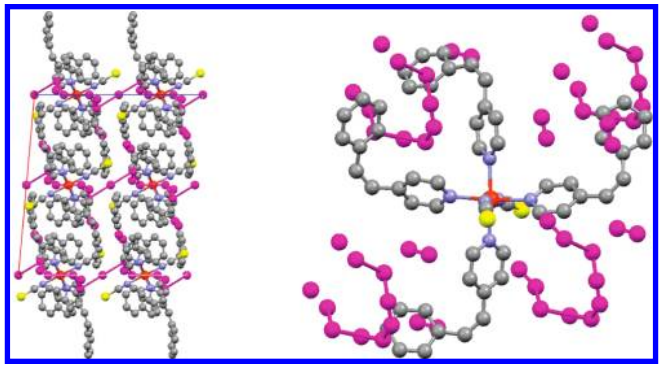

Figure 5. Position of the free cavity space (purple spheres) within the all-cis reactant matrix. (left) Structure projected along the *b* crystallographic axis. (right) Free cavities in the neighborhood of a central all-cis molecule.

(Tables S1−S3 and Figure S4 in the Supporting Informations). The analysis of this crystal structure reveals the buildup of static disorder in parallel to the phototransformation, leading finally to an amorphous state.

A close inspection at the distribution of the free cavity space within the crystal lattice of the all-cis reactant material may help in understanding the possible cis-to-trans photoisomerization. As is evident in Figure 5, the cavity spaces, defined as the region of the unit-cell that could accommodate probe spheres of a 0.8 Å radius not entering the van der Waals surfaces of neighboring atoms, are distributed in a nonsystematic manner with respect to the phenyl rings of the stpy ligands.

To facilitate a cis-to-trans isomerization, we could expect the free cavities to be mostly located around the phenyl rings of the stpy ligands, at least at the putative position of the phenyl ring after cis-to-trans isomerization. This is clearly not the case in the present material as shown in Figure 5. In conclusion, a single-crystal-to-single-crystal photoisomerization is not likely to occur. This may be the reason why the phototransformation leads to an amorphous solid.

The unit-cell expansion and the solid amorphization observed here by X-ray diffraction are two features that might stabilize a HS phase.[35] We have performed optical and photomagnetic measurements for probing the thermal behavior of the photogenerated species to confirm this hypothesis.

3. Impact of Stpy *Z* → *E* Isomerization on the Fe^{II} Electronic Properties. ***a. Variable-Temperature Diffuse Reflectivity Measurements.*** As shown in Figure S5 (Supporting Informations), the reflectivity of the all-cis solid only slightly varies between 80 and 300 K (0.76−0.78) as expected for a HS species. On the contrary, for the all-trans solid, the much larger variation of ~0.13 observed between 220 and 130 K is consistent with a thermal spin crossover. Indeed, the HS fraction curve (Figure 6), extracted from the reflectivity data by using the Kubelka−Munck formula,[25] compares well with the magnetic measurements (Figure S6, Supporting Informations).

The red product formed at RT by irradiating the orange HS all-cis compound (532 nm, 600 min) is characterized by a distinctive reflectivity variation similar to the one of the all-trans solid, suggesting a thermal spin-crossover for this material as well.

For comparison, we have in a first approximation extrapolated the low-temperature limit of the reflectivity values and, as detailed above for the all-trans isomer, we have determined the HS fraction curve of the photoproduct (Figure 6 left). The resulting gradual curve of the photoproduct is centered at a temperature of ~116 K, lower than the half transition of the all-trans isomer (at 166 K). The spin-crossover characteristics seem to be consistent with the strengthening of the ligand-field

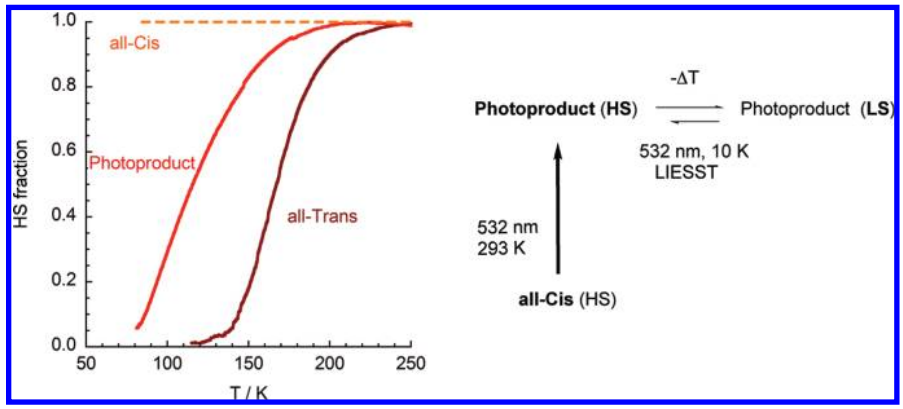

Figure 6. (left) HS fraction vs temperature extracted from diffuse reflectivity measurements. For comparison, a horizontal line is drawn at $\gamma_{HS} = 1$ for the all-cis sample. (right) Scheme of the reactions investigated for the all-cis sample.

on going from the all-cis reactant to the photoproduct and then to the all-trans reference.

b. Low-Temperature Photomagnetic Measurements Based on the LIESST Effect. If, as suggested by the variable-temperature reflectivity measurements, HS and LS species coexist within the photoproduct in a thermal equilibrium (i.e., spin crossover occurs), then the photoexcitation based on the LIESST effect might possibly be achieved, for example at 10 K, and detected by magnetic measurements. A small amount of all-cis solid was first illuminated at RT with a 532 nm light to generate the photoisomerized product. After saturation of the IR signal showing the stpy isomerization, the sample was cooled to 10 K within the magnetometer. The magnetization was then recorded as a function of time before and after the in situ excitation at 532 nm (inactive at low temperature with respect to isomerization). The evolution (Figure S7, Supporting Informations) was typical of a photoexcitation (positive magnetization variation indicating the LS to HS conversion) followed by a 10 K relaxation process (slow decay of magnetization in the dark toward the initial value corresponding to the LS ground state). This LIESST study confirms the presence of LS species at 10 K and correlatively confirms a spin-crossover process for the photoproduct (Figure 6, right).

In summary, the ligand-centered reaction carried out at RT in a densely packed solid is shown to drive a detectable change in the spin-state energies of the metal ion, which is the prerequisite for the LD-LISC effect.

4. Excited States of the Styrylpyridine: Computation of the Triplet−Singlet Energy Difference. As will be discussed later, we have focused on the photoreactivity of the free-base ligands for analyzing our experimental results. It is easily checked that the stpy isomers do not react in solution under a 550 nm excitation. This observation agrees with the experimental and theoretical investigations of stpy isomerization showing a high-energy singlet pathway at RT. A triplet pathway via $^3\pi\pi^*$ excited states at lower energies also exists; it is barrierless and actually requires sensitization, low-temperature, or heavy-atom effects.[36] The corresponding triplet−singlet energy differences have been calculated and the results are summarized in Table 1.

For the cis- and trans-isomers in their ground-state geometries, the vertical T_1/S_0 electronic excitation energies are 24279 and 21141 cm^{-1}, respectively. Upon geometry relaxation in the T_1 state, we have found T_1/S_0 zero-point energy differences of 13661 and 16565 cm^{-1}, for the cis- and trans-isomers, respectively. This zero-point energy difference found for the trans-isomer is in very good agreement with the value of about 17500 cm^{-1} determined experimentally by Görner for this isomer in various glassy media.[37] This makes us quite confident about the quality of the results obtained for the characterization of the T_1/S_0 energy differences in the 4-stpy free-base.

TABLE 1: T_1/S_0 Energy Differences for the Cis- and Trans-Isomers of 4-Styrylpyridine: Vertical Electronic Energy Differences $\Delta E_{T/S}$ at the Cis and Trans Ground-State Minima and Zero-Point Energy Differences $\Delta E_{T/S}^0$ (in cm^{-1}; B3LYP/DZVP results)[a]

	cis-isomer	trans-isomer
$\Delta E_{T/S}$	24279	21141
$\Delta E_{T/S}^0$	13661[b]	16565
$\Delta E(^5\text{MLCT}^*)$	~23000	~22000

[a] Experimental values corresponding to the ^{5}MLCT excited state of the related complexes are reported for comparison. [b] The relaxed geometry found for the cis isomer in the T_1 state proves to be the T_1-state perpendicular geometry (i.e., with the phenyl and pyridinyl groups perpendicular). No other extremum could be found for this isomer in this state. This agrees with the fact that no barrier to the torsion about the central ethylenic bond in the T_1 state was reported.

IV. Discussion

On the Solid-State Reactivity. We have shown the occurrence of a styrylpyridine isomerization in the crystalline all-cis solid that does not proceed through a single-crystal-to-single-crystal transformation. For taking into account the significant misfit of the free cavity locations in the crystal packing, it seems appropriate to propose the volume-conserving hula-twist as an alternative mechanism.[17] Despite comparable absorption properties of all-cis and all-trans solids in the 500−550 nm range, we have characterized a unidirectional cis-to-trans conversion under visible excitation. Unidirectional reactivity was reported for several bis(biphenyl)ethylenes and ethenes in the solid state.[38] The general observation that unidirectional photoisomerization reactions occur from the more dense to the less dense crystal packing is verified here: a gradual unit-cell volume expansion has been derived from the crystallographic analysis upon laser exposure. The inactive all-trans complex contains four distinct stpy ligands and thus the very low symmetry of complex produces different excited states, pathways, and clearly energy barriers with respect to the cis isomer. This reactivity can be attributed to the molecular photophysical characteristics (discussed hereafter) and/or environment effects in the solid state.

On the MLCT Pathway. The optical measurements establish that the low-energy excitation (500−650 nm) used for triggering the cis-to-trans isomerization of stpy corresponds to the Fe(3d)-to-π^* (stpy) charge transfer transition of the HS metal ion instead of a $\pi\pi^*$ transition. In coordination compounds, large

spin−orbit coupling between electronic states of different spin multiplicities strongly accelerates intersystem crossing (isc) and favors the triplet pathway, as evidenced for example in Re(I) or Ru(II) complexes.[11,39] Accordingly, one working hypothesis to consider here is an intersystem crossing from the ^{5}MLCT* state to the ligand-localized excited states. Note that, at this stage, a mechanism involving an intermolecular energy transfer (or an electron transfer) cannot be discarded.

For the triplet pathway to be plausible in the present case, the ^{5}MLCT states of the HS complex must be above or close in energy to the intraligand excited state, which can be identified as the T_1 state of the stpy free-base, and which we will denote ^{3}IL(stpy). In Table 1 are reported the calculated values for the T_1/S_0 energy differences in 4-styrylpyridine as well as the experimental energy values corresponding to the ^{5}MLCT excited states of the related complexes. From this, the ^{5}MLCT absorption band of the Fe(II) all-cis complex being centered at ca. 23000 cm^{-1}, the results obtained for the T_1/S_0 energetics indicate that the conditions on the relative positions of the ^{5}MLCT and ^{3}IL(stpy) states are fulfilled for the photoisomerization to take place in the ^{3}IL(stpy) state. That is, upon photoexcitation into the ^{5}MLCT manifold, the ^{3}IL(stpy) may be populated by ISC and the isomerization of the ligand can then take place from this state.

One further condition for the triplet pathway to occur is that this reaction is fast enough to compete with the decay of a ^{5}MLCT excited state characterizing a Fe^{II} compound. To the best of our knowledge, the relaxation mechanism of ^{5}MLCT excited states of iron(II) complexes has not been reported so far. The recent photophysical studies of iron(II) compounds have focused on the excitation of $Fe^{II}(bpy)_3^{2+}$, a LS model of spin-crossover systems in solution.[40] These studies combined with the solid-state LIESST experiments performed by Hauser[4] have identified relaxation processes toward the ground state (GS) depending on the initially excited state: ^{1,3}MLCT → ^{5}T → ^{1}GS (MLCT) and ^{1}T → ^{3}T → ^{5}T → ^{1}GS (ligand-field).

Additional investigations are presently required for rationalizing the reaction pathway between the MLCT and the ligand-localized excited states.

On the LD-LISC Effect. The photoswitching of the all-cis solid suggests some comments. The photoproduct exhibits a thermal spin-crossover process while the all-cis reactant remains in the HS state at all temperatures. This drastic evolution contrasts with the expectation of a relative stabilization of the HS state favored in spin-crossover materials by a unit-cell expansion, solid disorder, or amorphization.[35] However, this evolution is in qualitative agreement with the magnetic properties of the references (bulk samples, compounds dispersed in PMMA) and also the photomagnetic LD-LISC effect observed in PMMA thin films (specific conditions, $T = 130$ K and $\lambda = 355$ nm). The *cis*-styryl isomerization produces a strengthening of the ligand field, which in turn switches the metal ion's spin state energies to give a thermal spin-crossover.

Another point is the observation of a transition curve centered at a lower temperature than the curve of the pure all-trans species. In fact, the shape of the thermal dependence of the HS fraction curve of the photoproduct constitutes an envelope of several curves resulting from complexes with cis- and trans-ligand isomers. This result agrees with the amorphous character of the product and also the formation of complexes with disordered positions of stpy as concluded from the crystallographic analysis of the photoperturbed crystalline phase (see above and the Supporting Informations).

Finally, the synergy between the spin state of the metal ion and the ligand-centered reaction, i.e. the so-called LD-LISC effect, may be investigated at a working temperature below ca. 160 K. These developments will be reported elsewhere in a forthcoming work.

V. Conclusions

The cis → trans photoisomerization of stilbenoids is here demonstrated for the very first time in a crystalline inorganic compound. The reaction occurs in a unidirectional manner under the effect of an excitation in a MLCT band located in the visible range. From the crystallographic observations, it is obvious that the isomerization induced by visible light in the crystalline solid state proceeds in a nontopotactic manner, with progressive crystal disintegration, probably related to the characterized unit-cell volume expansion and the parallel buildup of internal strain. The key points are the presence of a bulky coordination group and the occurrence of twisted conformations preventing direct π-stacking associations, both factors providing a large fraction of free-cavities volumes. For explaining this reactivity, the volume-conserving hula-twist mechanism appears as the more reasonable hypothesis. The distinctive behaviors of all-cis and all-trans isomers are hardly assignable to the unique structural properties and thus, we believe that competitive photophysical processes and/or energy barrier might occur with the *trans*-styryl isomer, providing the unidirectional character of the reaction. Remarkably, this solid-state transformation is triggered by a low-energy ^{5}MLCT excitation. From our DFT calculations on the free-base ligands, we suggest that the photoexcitation into the ^{5}MLCT manifold may lead to the population of the ^{3}IL (stpy) state and then to the photoisomerization from this state.

The studied inorganic compounds present interesting photochemical behaviors that highlight the key role of media and working parameters. The spin change of the metal ion driven by the ligand photoswitching was previously reported in PMMA thin films. The bidirectional transformation has required highly diluted thin films for a mechanism activated by UV irradiation. In the present work, we have evidenced an effect related to LD-LISC in a dense crystalline media that requires an indirect and low-energy MLCT pathway. We have mainly focused on the crystallographic and optical properties of the iron(II) compounds for identifying the processes involving the organic and inorganic moieties in the solid phase. To complement these results, we plan to investigate (i) the interplay between the photoisomerization and the change of metal ion spin states (the LD-LISC effect) by variable-temperature reflectivity and magnetic measurements, (ii) the reaction kinetics of these coupled processes, and (iii) the photophysical aspects.

Application of this approach to systems incorporating photochromic functions like diarylethene or diazobenzene appears especially interesting as for these latter,[41−43] the structural reorganizations associated with the photoisomerization are limited and the large photochromism allows the different chromophores to be specifically addressed.

Acknowledgment. We thank Dr. Davy Loutete-Dangui and Prof. René Clément for their assistance and Prof. Andreas Hauser for discussions. The support provided by the CNRS, the French Ministry of Research (PPF "Cristallographie et Photocristallographie à haute résolution" and PPF "Photocommutation à l'Etat Solide"), the ANR (contract no. NT09-3-548342), the PRES UniverSud (COPECS Project), and the Swiss National Supercomputing Centre (CSCS) for the calculation resources allocated under project ID 103 is acknowledged. The

authors also thank the GDR 3053: "Magnétisme et Commutation Moléculaire" and MAGMANet NoE of the European Union (contract NMP3-CT-2005-515767-2).

Supporting Information Available: Refractive index spectra, ATR-IR spectra, and VT-diffuse reflectivity data (all-cis, all-trans references and photoproduct), the HS fraction vs T curves extracted from magnetic and reflectivity data (all-trans compound), LIESST effect shown by the photoproduct, and tables of structural parameters and molecular structure of the all-cis phase after photoexcitation. This material is available free of charge via the Internet at http://pubs.acs.org.

References and Notes

(1) Kahn, O. *Molecular Magnetism*; Wiley-VCH: New York, 1993.
(2) *Topics in Current Chemistry*; Gütlich, P., Goodwin, H. A., Eds.; Springer: Berlin, Germany, 2004; Vols. 233−235.
(3) Létard, J.-F. In *Topics in Current Chemistry*; Gütlich, P., Goodwin, H. A., Eds.; Springer: Berlin, Germany, 2004; Vol. 235, p 221.
(4) Hauser, A. In *Topics in Current Chemistry*; Gütlich, P., Goodwin, H. A., Eds.; Springer: Berlin, Germany, 2004; Vol. 234, p 155.
(5) (a) Roux, C.; Zarembowitch, J.; Gallois, B.; Granier, T.; Claude, R. *Inorg. Chem.* **1994**, *33* (10), 2273–2279. (b) Boillot, M.-L.; Roux, C.; Audière, J. P.; Dausse, A.; Zarembowitch, J. *Inorg. Chem.* **1996**, *35*, 3975–3980. (c) Roux, C.; Zarembowitch, J. *New J. Chem.* **1992**, *16*, 671–677.
(6) (a) Boillot, M.-L.; Zarembowitch, J.; Sour, A. In *Topics in Current Chemistry*; Gütlich, P., Goodwin, H. A., Eds.; Springer: Berlin, Germany, 2004; Vol. 234, p 261. (b) Boillot, M.-L.; Chantraine, S.; Zarembowitch, J.; Lallemand, J. Y.; Prunet, J. *New J. Chem.* **1999**, *23*, 179–183.
(7) Lawson-Daku, L. M.; Linarès, J.; Boillot, M.-L. *ChemPhysChem.* **2007**, *8*, 1402–1416.
(8) (a) Sato, O. *Acc. Chem. Res.* **2003**, *36*, 692–700. (b) Létard, J.-F. *J. Mater. Chem.* **2006**, *16*, 2550–2559. (c) Shimizu, H.; Okubo, M.; Nakamoto, A.; Enomoto, M.; Kojima, N. *Inorg. Chem.* **2006**, *45*, 10240–10247. (d) Kojima, N.; Okubo, M.; Shimizu, H.; Enomoto, M. *Coord. Chem. Rev.* **2007**, *251*, 2665–2673. (e) Bleuzen, A.; Marvaud, V.; Mathonière, C.; Sieklicka, B.; Verdaguer, M. *Inorg. Chem.* **2009**, *48*, 3453–3466. (f) Paquette, M. M.; Kopelman, R. A.; Beitler, E.; Frank, N. L. *Chem. Commun.* **2009**, 5424–5426. (g) Kida, N.; Hikita, M.; Kashima, I.; Okubo, M.; Itoi, M.; Enomoto, M.; Kato, K.; Takata, M.; Kojima, N. *J. Am. Chem. Soc.* **2009**, *131*, 212–220. (h) Wang, M.-S.; Xu, G.; Zhang, Z.-J.; Guo, G.-C. *Chem. Commun.* **2010**, *46*, 361–376.
(9) (a) Meier, H. *Angew. Chem., Int. Ed. Engl.* **1992**, *31*, 1399–1420. (b) Feringa, B. L.; Jager, W. F.; Delange, B. *Tetrahedron* **1993**, *49*, 8267–8310.
(10) (a) Balzani, V.; Credi, A.; Raymo, F. M.; Stoddart, J. F. *Angew. Chem., Int. Ed.* **2000**, *39*, 3348–3391. (b) Feringa, B. L. *Molecular Switches*: Wiley-VCH: Weinheim, Germany, 2001. (c) Amimoto, K.; Kawato, T. *J. Photochem. Photobiol., C* **2005**, *6*, 207–226. (d) Irie, M. *Bull. Chem. Soc. Jpn.* **2008**, *81*, 917–926.
(11) (a) Vlcek, A.; Busby, M. *Coord. Chem. Rev.* **2006**, *250*, 1755–1762. (b) Bossert, J.; Daniel, C. *Chem.—Eur. J.* **2006**, *12*, 4835–4843.
(12) Soyer, H.; Mingotaud, C.; Boillot, M.-L.; Delhaes, P. *Langmuir* **1998**, *14*, 5890–5895.
(13) Kolb, J. S.; Thomson, M. D.; Novosel, M.; Sénéchal-David, K.; Rivière, E.; Boillot, M.-L.; Roskos, H. G. *C. R. Chim.* **2007**, *10*, 125–136.
(14) Boillot, M.-L.; Pillet, S.; Tissot, A.; Rivière, E.; Claiser, N.; Lecomte, C. *Inorg. Chem.* **2009**, *48*, 4729–4736.
(15) (a) Gütlich, P.; Garcia, Y.; Woike, T. *Coord. Chem. Rev.* **2001**, *219*, 839–879. (b) Varret, F.; Nogues, M.; Goujon, A. In *Magnetism: Molecules to Materials*; Miller, J., Drillon, M., Eds.; Wiley VCH: Weinheim, Germany, 2001; Vol. II, p 257.
(16) Martinez, T. J. *Acc. Chem. Res.* **2006**, *39*, 119–126.
(17) Liu, R. S. H.; Hammond, G. S. *Acc. Chem. Res.* **2005**, *38*, 396–403.
(18) Fuss, W.; Kosmidis, C.; Schmid, W. E.; Trushin, S. A. *Angew. Chem., Int. Ed.* **2004**, *43*, 4178–4182.
(19) Moorthy, J. N.; Venkatakrishnan, P.; Savitha, G.; Weiss, R. G. *Photochem. Photobiol. Sci.* **2006**, *5*, 903–913.
(20) (a) Kaupp, G.; Haak, M. *Angew. Chem., Int. Ed. Engl.* **1996**, *35*, 2774–2777. (b) Kaupp, G. *Curr. Opin. Solid State Mater. Sci.* **2002**, *6*, 131–138.
(21) Zheng, S.-L.; Vande Velde, C. M. L.; Messerschmidt, M.; Volkov, A.; Gembicky, M.; Coppens, P. *Chem.—Eur. J.* **2008**, *14*, 706–713.
(22) (a) Humlicek, J.; Schmidt, E.; Bocanek, L.; Svehla, R.; Ploog, K. *Phys. Rev. B.* **1993**, *48*, 5241–5248. (b) Azzam, R. M. A.; Bashara, N. M. *Ellipsometry and Polarized Light*; North-Holland: Amsterdam, The Netherlands, 1977.
(23) (a) Toll, J. S. *Phys. Rev.* **1956**, *104*, 1760–1770. (b) Landau, L. D.; Lifshitz, E. M. *Electrodynamics of continuous media*; Pergamon Press: New York, 1963. (c) Stern, F. *Solid State Phys.* **1963**, *15*, 299–408.
(24) Loutete-Dangui, E. D.; Varret, F.; Codjovi, E.; Dahoo, P. R.; Tokoro, H.; Ohkoshi, S.; Eypert, C.; Létard, J.-F.; Coanga, J. M.; Boukheddaden, K. *Phys. Rev. B* **2007**, *75*, B184425.
(25) (a) Morscheidt, W.; Jeftic, J.; Codjovi, E.; Linares, J.; Bousseksou, A.; Constant-Machado, H.; Varret, F. *Meas. Sci. Technol.* **1998**, *9*, 1311–1315. (b) Jeftic, J.; Menendez, N.; Wack, A.; Codjovi, E.; Linares, J.; Goujon, A.; Hamel, G.; Klotz, S.; Syfosse, G.; Varret, F. *Meas. Sci. Technol.* **1999**, *10*, 1059–1064. (c) Jeftic, J.; Kindler, U.; Spiering, H.; Hauser, A. *Meas. Sci. Technol.* **1997**, *8*, 479–483. (d) Tanasa, R.; Stancu, A.; Létard, J.-F.; Codjovi, E.; Linares, J.; Varret, F. *Chem. Phys. Lett.* **2007**, *443*, 435–438.
(26) Lebedev, G.; Pillet, S.; Baldé, C.; Guionneau, P.; Desplanches, C.; Létard, J.-F. *IOP Conf. Ser.: Mater. Sci. Eng.* **2009**, *5*, 012025.
(27) (a) Hohenberg, P.; Kohn, W. *Phys. Rev.* **1964**, *136*, B864. (b) Kohn, W.; Sham, L. J. *Phys. Rev.* **1965**, *140*, A1133.
(28) (a) NWChem Version 5.1.1, as developed and distributed by Pacific Northwest National Laboratory, P.O. Box 999, Richland, WA 99352, USA, and funded by the U.S. Department of Energy. (b) Kendall, R. A.; Aprà, E.; Bernholdt, D. E.; Bylaska, E. J.; Dupuis, M.; Fann, G. I.; Harrison, R. J.; Ju, J.; Nichols, J. A.; Nieplocha, J.; Straatsma, T. P.; Windus, T. L.; Wong, A. T. *Comput. Phys. Commun.* **2000**, *128*, 260–283.
(29) (a) Becke, A. D. *J. Chem. Phys.* **1993**, *98*, 1372–1377. (b) Becke, A. D. *J. Chem. Phys.* **1993**, *98*, 5648–5652. (c) 33 Gaussian NEWS, v. 5, no. 2, summer 1994, p 2, Becke3LYP Method References and General Citation Guidelines.
(30) Godbout, N.; Salahub, D. R.; Andzelm, J.; Wimmer, E. *Can. J. Chem.* **1992**, *70*, 560–571.
(31) Lawson Daku, L. M.; Linares, J.; Boillot, M.-L. *Phys. Chem. Chem. Phys.* **2010**, *12*, 6107–6123.
(32) (a) Toftlund, H. *Coord. Chem. Rev.* **1989**, *94*, 67–108. (b) Sénéchal-David, K.; Zaman, N.; Walko, M.; Halza, E.; Rivière, E.; Guillot, R.; Feringa, B. L.; Boillot, M.-L. *Dalton Trans.* **2008**, *14*, 1932–1936.
(33) It is noteworthy that ellipsometry collects information on sample layers situated in some penetration depth given in a first approximation by $\delta = 1/\alpha(\lambda) = \lambda/4\pi k(\lambda)$. The latter depends on the wavelength and gives $\delta \approx 50$ (280) nm for $\pi\pi^*$ (MLCT) absorption band of the all-cis compound.
(34) Tuchagues, J.-P.; Bousseksou, A.; Molnar, G.; McGarvey, J. J.; Varret, F. In *Topics in Current Chemistry*; Gütlich, P., Goodwin, H. A., Eds.; Springer: Berlin, Germany, 2004; Vol. 235, p 85.
(35) (a) Haddad, M. S.; Federer, W. D.; Lynch, M. W.; Hendrickson, D. N. *Inorg. Chem.* **1981**, *20*, 131–139. (b) Martin, J.-P.; Zarembowitch, J.; Bousseksou, A.; Dworkin, A.; Haasnoot, J. G.; Varret, F. *Inorg. Chem.* **1994**, *33*, 6325–6333. (c) Constant-Machado, H.; Linarès, J.; Varret, F.; Haasnoot, J. G.; Martin, J.-P.; Zarembowitch, J.; Dworkin, A.; Bousseksou, A. *J. Phys. I* **1996**, *6*, 1203–1216.
(36) Barigelleti, F.; Dellonte, S.; Orlandi, G.; Bartocci, G.; Masetti, F.; Mazzucato, U. *J. Chem. Soc., Faraday Trans.* **1984**, *80*, 1123–1129.
(37) Görner, H. *J. Phys. Chem.* **1989**, *93*, 1826–1832.
(38) Zhu, F. Q.; Motoyoshiya, J.; Nishii, Y.; Aoyama, H.; Kakehi, A.; Shiro, M. *J. Photochem. Photobiol., A* **2006**, *184* (1−2), 44–49.
(39) (a) Shaw, J. R.; Webb, R. T.; Schmehl, R. H. *J. Am. Chem. Soc.* **1990**, *112*, 1117–1123. (b) Zarnegar, P. P.; Bock, C. R.; Whitten, D. G. *J. Am. Chem. Soc.* **1973**, *95* (13), 4367–4372.
(40) Cannizo, A.; Milne, C. J.; Consani, C.; Gawelda, W.; Bressler, C.; Van Mourik, F.; Chergui, M. *Coord. Chem. Rev.* **2010**, *254*, 2677–2686.
(41) Matsuda, K.; Takayama, K.; Irie, M. *Inorg. Chem.* **2004**, *43*, 482–489.
(42) Hasegawa, Y.; Kume, S.; Nishihara, H. *Dalton Trans.* **2009**, *2*, 280–284.
(43) Kume, S.; Nishihara, H. *Struct. Bonding (Berlin)* **2007**, *123*, 79–112.

JP106583F